Quantitative Comparison of Self-Consistent Field Theories for Polymers near Interfaces with Monte Carlo Simulations

Friederike Schmid* and Marcus Müller

Johannes Gutenberg Universität Mainz, D55099 Mainz, Germany

Received May 23, 1995; Revised Manuscript Received August 1, 1995®

ABSTRACT: A planar interface between immiscible phases in a symmetric polymer blend is studied in self-consistent field theory for completely flexible (Gaussian) and semiflexible (wormlike) chains. Concentration and density profiles, chain end distributions, interfacial tensions, and the orientational order of whole chains and single monomers are calculated. The results are compared with data from Monte Carlo simulations. The qualitative agreement is overall very good. Quantitatively, the theory succeeds in predicting the correct profile widths only in the limit of extremely long chain lengths, and only for small values of the Flory–Huggins parameter χ.

1. Introduction

Polymer blends are often considered as an example for a physical system which can be accurately described by a mean field type theory. In the limit of high molecular weight, one polymer interacts with many others, and the mean field approximation can be justified by a simple Ginzburg type self-consistency criterion.[1,2]

On the other hand, polymer blends are seldom homogeneous on a mesoscopic scale. Organic molecules of different types tend to demix at low temperatures. For polymers, the demixing temperature is very high, since the internal energy connected with the relative repulsion of unlike polymer segments is proportional to the total number of segments and thus completely dominates the entropy of mixing, which is proportional to the number of molecules. Polymer blends can therefore often be described as assemblies of interfaces between essentially unmixed phases, and the properties of those materials are to a great extent governed by the properties of the interfaces.[3]

Among other elaborated mean field approaches to the study of such inhomogeneous polymeric systems (see, e.g., refs 3–6), the powerful tool of the self-consistent field theory has been developed by Helfand and coworkers[7,8] and subsequently applied to various systems of special interest, such as polymer brushes and copolymer mesophases.[9,10] The main idea behind this approach consists of treating the polymer as a random walk in a position dependent chemical potential, which depends self-consistently on the distribution of monomers. The chains are mostly considered to be completely flexible (Gaussian chains). Much less work has been done on inhomogeneous systems of semiflexible polymers (wormlike chains); however, the extension of the theory to this more general case is relatively straightforward.[11]

This type of theory is generally believed to provide a fairly accurate description of real systems, even quantitatively. However, their use still requires some caution. Close to the critical (demixing) point, the system is governed by large concentration fluctuations, and mean field behavior is reached only for very long chain lengths, with an extended crossover regime to Ising behavior.[12–14] Far below the critical point, the interface width becomes comparable with characteristic microscopic length scales of the system, and the interface cannot be described in terms of idealized coarse-grained models any more.

The limitations of mean field theories can most directly be explored by quantitative comparison with experimental[16] or simulation data.[18] The latter approach has the advantage that one compares with a precisely defined system, without undetermined parameters. However, simulation studies of inhomogeneous polymeric systems are computationally extremely demanding.[19] Only recently has one of us—using a massively parallel CRAY-T3D system—been able to perform large scale simulations of the interface between two immiscible phases of a symmetric polymer mixture.[20] The bulk properties of the model are very well-known from previous work,[12,21–23] and the structure of the interface could be studied in great detail. These simulations provide an excellent base for a comparison with self-consistent field theories.

In the present work, we employ Helfand's theory for inhomogeneous systems of Gaussian chains,[8] as well as its extension for semiflexible chains,[11] to study an interface with parameters chosen such that it corresponds directly to the simulated interface. In other work additional assumptions are often made, e.g. that the polymer size is much larger than the interface width (strong segregation limit[7]), or much smaller (weak segregation limit[24]). Here, we solve the self-consistent field equations numerically without resorting to further approximations (cf. ref 15). Moreover, we have no adjustable parameters. Thus our results allow for a direct, quantitative comparison of interfacial properties in self-consistent field theory and in the simulated model.

Our paper is organized as follows. In the next section, we review the self-consistent field theory for Gaussian and semiflexible chains and reformulate the latter in a way that enables us to solve it numerically. In section 3, we describe the bond fluctuation model for polymers which was used in the Monte Carlo simulations. The results are compared in section 4 and summarized in the last section.

® Abstract published in *Advance ACS Abstracts,* November 1, 1995.

0024-9297/95/2228-8639$09.00/0

2. Self-Consistent Field Theory

We consider an interface between two coexisting phases in a mixture of polymer species A and B. Each chain of type i (i = A or B) contains N_i monomers and is characterized by either only a statistical segment length b_i (Gaussian chains) or a fixed monomer length, a_i and a dimensionless stiffness η_i (semiflexible chains)—in this case, we have $b_i = \sqrt{2\eta_i}a_i$. In the homogeneous melt, these parameters relate the end to end distance R_e of the polymer with the degree of polymerization N via $R_e^2 = b_i^2(N-1)$ (random walk). We will restrict ourselves to the symmetric case, where N, η, b, and a are equal for both species and the monomer density ϱ in the two phases is the same.

Molecules will be treated as space curves $\vec{r}(s)$, with s varying from 0 to 1. The partition function we use for a system of n_A polymers of type A and n_B polymers of type B has the general form[8]

$$\mathcal{Z} = \frac{1}{n_A!n_B!}\int\prod_{i=1}^{n_A}\hat{\mathcal{D}}\{\vec{r}_i(\cdot)\}\prod_{j=1}^{n_B}\hat{\mathcal{D}}\{\vec{r}_j(\cdot)\}\,\exp[-\beta\mathcal{H}\{\hat{\Phi}_A,\hat{\Phi}_B\}] \tag{1}$$

where $\beta = 1/k_BT$ is the Boltzmann factor and $\hat{\Phi}_A$ and $\hat{\Phi}_B$ are dimensionless monomer density operators

$$\hat{\Phi}_{A,B}(\vec{r}) = \frac{N}{\varrho}\sum_{i=1}^{n_{A,B}}\int_0^1 ds\;\delta(\vec{r}-\vec{r}_i(s)) \tag{2}$$

and $\mathcal{H}\{\hat{\Phi}_A,\hat{\Phi}_B\}$ represents a coarse-grained free energy functional of the form

$$\beta\mathcal{H} = \varrho\int d\vec{r}\; f_{Int}\{\hat{\Phi}_A,\hat{\Phi}_B\} + f_{FV}\{\hat{\Phi}_A,\hat{\Phi}_B\}] \tag{3}$$

The energetic contribution can be written as $f_{Int} = \sum_{i,j}\chi_{ij}\hat{\Phi}_i\hat{\Phi}_j$, and several forms have been proposed for the free volume contribution f_{FV}.[26,27] Here, we deal with the limit of a dense, almost incompressible melt with a total density varying by no more than a few percent throughout the interface. Hence we can use the simple quadratic approximation introduced by Helfand

$$\beta\mathcal{H} = \varrho\int d\vec{r}\;\left\{\chi\hat{\Phi}_A(\vec{r})\hat{\Phi}_B(\vec{r}) + \frac{\zeta}{2}(\hat{\Phi}_A(\vec{r}) + \hat{\Phi}_B(\vec{r}) - 1)^2\right\} \tag{4}$$

with the Flory–Huggins parameter χ measuring the relative repulsion between species A and B, and a parameter $1/\zeta = \varrho k_BT\kappa$, which is proportional to the compressibility κ of the melt. The results (Figure 7) show that the approximation works fairly well for the system in question.

In this formalism, systems of Gaussian or semiflexible chains differ from each other in the statistical weight $\mathcal{P}_W$, which is assigned to the individual space curves in the functional integral: $\hat{\mathcal{D}}\{\vec{r}(\cdot)\} = \mathcal{D}\{\vec{r}(\cdot)\}\,\mathcal{P}_W\{\vec{r}(\cdot)\}$ with

$$\mathcal{P}_W\{\vec{r}(\cdot)\} = \mathcal{N}\exp\left[-\frac{3}{2Nb^2}\int_0^1 ds\,\left|\frac{d\vec{r}}{ds}\right|^2\right] \tag{5}$$

for Gaussian chains,[8] and

$$\mathcal{P}_W\{\vec{r}(\cdot)\} = \mathcal{N}\prod_s\delta(\vec{u}^2-1)\exp\left[-\frac{\eta}{2N}\int_0^1 ds\,\left|\frac{d\vec{u}}{ds}\right|^2\right] \tag{6}$$

for semiflexible chains.[28] Here $\vec{u} = (d\vec{r}/ds)/(Na)$ is a dimensionless tangent vector constrained to unity by the delta function and $\mathcal{N}$ is the normalization factor. Gaussian chains are hence modeled as continuous space curves, which are distributed according to a Gaussian stretching energy with spring constant $3/Nb^2$. Semiflexible chains are treated as smooth space curves with a fixed segment length and a statistical weight based on an internal bending energy with bending rigidity η.

We solve the problem in mean field approximation by replacing the monomer density operator $\hat{\Phi}(\vec{r})$ in eq 4 with the average monomer density $\Phi_i(\vec{r}) \doteq \langle\hat{\Phi}_i(\vec{r})\rangle$. Monomer–monomer correlations are ignored. The chains can then be treated as independent random walks in the external field $W_i(\vec{r}) = \delta(\beta\mathcal{H})/\delta\Phi_i(\vec{r})$.[8] It is useful to define the end-segment distribution functions

$$Q_i(\vec{r}_0,s) = \int\hat{\mathcal{D}}\{\vec{r}(\cdot)\}\,\exp[-\int_0^s ds'\;W_i(\vec{r}(s'))]\delta(\vec{r}_0 - r(\vec{s})) \quad \text{(Gaussian chains)} \tag{7}$$

$$Q_i(\vec{r}_0,\vec{u}_0,s) = \int\hat{\mathcal{D}}\{\vec{r}(\cdot)\}\,\exp[-\int_0^s ds'\;W_i(\vec{r}(s'))]\delta(\vec{r}_0 - r(\vec{s}))\;\delta(\vec{u}_0 - u(\vec{s})) \quad \text{(semiflexible chains)} \tag{8}$$

which obey the diffusion equations[7,11]

$$\left\{\frac{1}{N}\frac{\partial}{\partial s} - \frac{1}{6}b^2\vec{\nabla}_{\vec{r}}^2 + W_i\right\}Q_i(\vec{r},s) = 0 \quad \text{(Gaussian)} \tag{9}$$

$$\left\{\frac{1}{N}\frac{\partial}{\partial s} + a\vec{u}\vec{\nabla}_{\vec{r}} - \frac{1}{2\eta}\vec{\nabla}_{\vec{u}}^2 + W_i\right\}Q_i(\vec{r},\vec{u},s) = 0 \quad \text{(semiflexible)} \tag{10}$$

with initial condition $Q_i(\vec{r},0) \equiv 1$ [$Q_i(\vec{r},\vec{u};0) \equiv 1$] and the Laplacian on the unit sphere $\nabla_{\vec{u}}^2$.

The function Q_i gives the statistical weight for a part of a polymer of type i and length sN, with one end fixed at position $\vec{r}$ (the tangent vector there being $\vec{u}$). The average density of type i monomers (with orientation $\vec{u}$) is then given by $\Phi_i(\vec{r}) = \int_0^1 ds\;Q_i(\vec{r},s)\,Q_i(\vec{r},1-s)$ [$\Phi_i(\vec{r},\vec{u}) = \int_0^1 ds\;Q_i(\vec{r},\vec{u},s)\,Q_i(\vec{r},-\vec{u},1-s)$], which completes the cycle of self-consistent equations.

Having solved them, one can calculate the chain end distribution $\Phi_{i,e}(\vec{r}) = Q_i(\vec{r},0)\,Q_i(\vec{r},1)$ and the configurational entropy for a polymer of type i

$$\mathcal{S}_i = k_B\left(\ln\mathcal{Z}_i + \frac{1}{n_i}\int d\vec{r}\;W_i(\vec{r})\,\Phi_i(\vec{r})\right) \tag{11}$$

where the single chain partition function $\mathcal{Z}_i = \int d\vec{r}\;Q_i(\vec{r},1) = Nn_i/\rho$ is a constant. Using (4), one obtains the free energy

$$\beta F = \beta\mathcal{H}\{\Phi_A,\Phi_B\} - \frac{1}{k_B}(n_A\mathcal{S}_A + n_B\mathcal{S}_B)$$

$$= -\varrho\chi\int d\vec{r}\;\Phi_A\Phi_B - \varrho\frac{\zeta}{2}\int d\vec{r}(\Phi_A + \Phi_B - 1)(\Phi_A + \Phi_B + 1) + \text{const} \tag{12}$$

For convenience, we switch to the dimensionless units $\tilde{r} = \vec{r}/(b/\sqrt{6\chi})$ and define $\tilde{\xi} = \zeta/\chi$ and $\tilde{\eta} = \eta\chi$. Since we consider a planar interface, we only have to solve the one-dimensional diffusion equations

$$\frac{1}{\chi N}\frac{\partial}{\partial s}Q_i(\hat{y},s) = \left\{\frac{\partial^2}{\partial \hat{y}^2} - \hat{W}_i\right\}Q_i(\hat{y},s) \quad \text{(Gaussian chains)} \quad (13)$$

$$\frac{1}{\chi N}\frac{\partial}{\partial s}Q_i(\hat{y},\hat{u},s) = \left\{-\sqrt{\frac{3}{\hat{\eta}}}\hat{u}\frac{\partial}{\partial \hat{y}} + \frac{1}{2\hat{\eta}}\left(\frac{\partial}{\partial \hat{u}}(1-\hat{u}^2)\frac{\partial}{\partial \hat{u}}\right) - \hat{W}_i\right\}Q_i(\hat{y},\hat{u},s)$$
(semiflexible chains) (14)

with suitable boundary conditions at $y \to \pm\infty$, where $\hat{u} = u_y$ is the y component of $\vec{u}$, and the fields $\hat{W}_i(\hat{y})$ are given by

$$\hat{W}_A(\hat{y}) = \Phi_B(\hat{y}) + \zeta(\Phi_A(\hat{y}) + \Phi_B(\hat{y}) - 1) \quad (15)$$

$$\hat{W}_B(\hat{y}) = \Phi_A(\hat{y}) + \zeta(\Phi_A(\hat{y}) + \Phi_B(\hat{y}) - 1) \quad (16)$$

For Gaussian chains, this problem can be solved numerically with relatively little computational effort. In the case of semiflexible chains, we proceed by expanding the functions Q_i in terms of Legendre polynomials, $Q_i(\hat{y},\hat{u},s) = \sum q_l^{(i)}(\hat{y},s)\,P_l(\hat{u})$, multiplying (14) with the nth Legendre polynomial $P_n(\hat{u})$, and integrating over $\hat{u}$. One gets the set of equations

$$\frac{1}{\chi N}\frac{\partial}{\partial s}q_n^{(i)}(\hat{y},s) = -\left\{\frac{1}{2\hat{\eta}}n(n+1) + \hat{W}_i(\hat{y})\right\}q_n^{(i)}(\hat{y},s) \quad (17)$$

with coefficients

$$C_{ln} = \frac{1}{2}\int_{-1}^{1}d\hat{u}\;\hat{u}P_l(\hat{u})\,P_n(\hat{u}) = \delta_{l,n+1}\frac{n+1}{4(n+1)^2-1} + \delta_{l,n-1}\frac{n}{4n^2-1} \quad (18)$$

and initial conditions $q_n^{(i)}(\hat{y},0) = \delta_{n,0}$, where δ is the Kronecker symbol. The monomer density in terms of the functions $q_l^{(i)}$ is then given by

$$\Phi_i(\hat{y}) = \sum_l(-1)^l\frac{1}{2l+1}\int_0^1 ds\; q_l^{(i)}(\hat{y},s)\,q_l^{(i)}(\hat{y},1-s) \quad (19)$$

In the limit of small chain rigidity $\hat{\eta}$, (17) implies that the amplitudes of $q_l^{(i)}$ decrease for increasing l following $q_{l+1}^{(i)} \propto [\sqrt{\hat{\eta}}/l(l+1)](\partial/\partial\hat{y})q_l^{(i)}(\hat{y}) + \mathcal{O}(\hat{\eta})$. In particular, one finds $q_1^{(i)} \approx -\sqrt{3\hat{\eta}}(\partial/\partial\hat{y})q_0^{(i)}(\hat{y})$. After inserting this into the equation for $q_0^{(i)}$, one gets

$$\frac{1}{\chi N}\frac{\partial}{\partial s}q_0^{(i)} = \frac{\partial^2}{\partial \hat{y}^2}q_0^{(i)} - \hat{W}_i(\hat{y})q_0^{(i)} \quad (20)$$

thus recovering the Gaussian limit for flexible chains. As one increases chain rigidity, more and more moments $q_l^{(i)}$ have to be taken into account. In this work, we had to include up to seven moments at the highest chain rigidities.

Our numerical method is a simple relaxation technique: The $(n+1)$th guess for $\hat{W}_i(y)$ is determined via $\hat{W}^{n+1} = \hat{W}^n + \lambda_n(\Delta\hat{W}^n)$, where $\Delta\hat{W}^n$ is the difference between the nth guess $\hat{W}^n$ and the field calculated from there using (13) or (17) and (15) and (16). The mixing parameter

$$\lambda_n = \min\left(0.1, \sqrt{\frac{(\hat{W}^n - \hat{W}^{n-1})^2}{(\Delta\hat{W}^n - \Delta\hat{W}^{n-1})^2}}\right) \quad (21)$$

varies between 0 and 0.1. Relative accuracy $\Gamma = \sum_i\int dy\,(\Delta\hat{W}_i)^2/\sum_i\int dy\,(\hat{W}_i)^2$ of 10^{-10} could generally be reached within a few hundred iteration steps. As boundary conditions, we chose $\hat{W}_i(\pm y_{max}) = \hat{W}_{i,bulk}^{\pm}$, where $\hat{W}_{i,bulk}^{\pm}$ denotes the bulk value of the fields in the two coexisting phases "+" and "−", and assumed $(\partial/\partial y)Q_i(\pm y_{max},s) = 0$.

We close this section with sketching the "strong segregation limit", which has been commonly studied in the literature. In the strong segregation approximation, chain end effects are neglected, and the left hand side of (13) and (14) is set to zero. For Gaussian chains and $\zeta \to \infty$, the problem can then be solved exactly and one gets a concentration profile $\Phi(\hat{y}) \propto \tanh(\hat{y})$.[7] Thus the width of the interface in this limit is given by $w_{SSL} = b/\sqrt{6\chi}$. For the interfacial tension, one finds $\beta\sigma_{SSL} = \sqrt{\chi/6}\rho b$.

3. Bond Fluctuation Model

The simulation method and most results for $N = 32$ have already been presented and discussed in detail elsewhere.[20] Here, we briefly describe the underlying model, focusing on the relationship between model parameters and the parameters of the self-consistent field theory.

In the bond fluctuation model, polymers are modeled as chains of effective monomers on a cubic lattice, each of which occupies a cube of eight neighboring sites, and which are connected by bond vectors of lengths $2 \le d \le \sqrt{10}$ (in units of lattice spacing). At volume fraction 0.5 or monomer density $\rho = {}^{0.5}/_{8} = {}^{1}/_{16}$, this model reproduces many properties of dense polymer melts; in particular, single chain configurations show almost ideal Gaussian chain statistics. We have two types of chains—A and B—whose monomers interact pairwise with interactions $\epsilon_{AA} = \epsilon_{BB} = -\epsilon_{AB} = -k_BT\epsilon$, if they are less than $\sqrt{6}$ lattice units apart from each other.

For the comparison with the self-consistent field theory, we need expressions for the parameters b, χ, and ζ. The statistical segment length b can be determined in the bulk phase using $b^2 = \langle R(l)^2\rangle/l$, where l denotes the distance of two monomers along the chain, and $R(l)$ their distance in space. In earlier work,[22] chains were shown to have ideal Gaussian statistics at volume fraction 0.5, down to the screening length of the excluded volume interaction $l_0 \approx 6$. The Flory–Huggins parameter χ can be calculated using $\chi = 2z\epsilon$, where z is the effective coordination number of a monomer, i.e. the average number of contacts with a monomer from a different chain. The inverse compressibility ζ is a little more difficult to obtain. Since the interactions between monomers are dominated by the effect of excluded volume, $z\epsilon \ll V_{excl} = 8$, we can use the relation $\zeta = \rho(\partial^2 s/\partial\rho^2)$, which is strictly valid for athermal systems. The entropy density s as a function of ρ has been determined in ref 23. One gets $\zeta \approx 4.1$.

The simulations were performed in an $L \times D \times L$ geometry at system size $D = 64$ and $L \le 512$, and chain lengths $N = 32$ and $N = 128$ with $L = 128$, $D = 128$. At $N = 32$, the bulk system is characterized by $b = 3.05$ and $z = 2.65$, and at $N = 128$, by $b = 3.16$ and $z = 2.35$. The value of z varies by less than 5% over the range of ϵ and is reduced by a small amount ($\le$10%) at the center

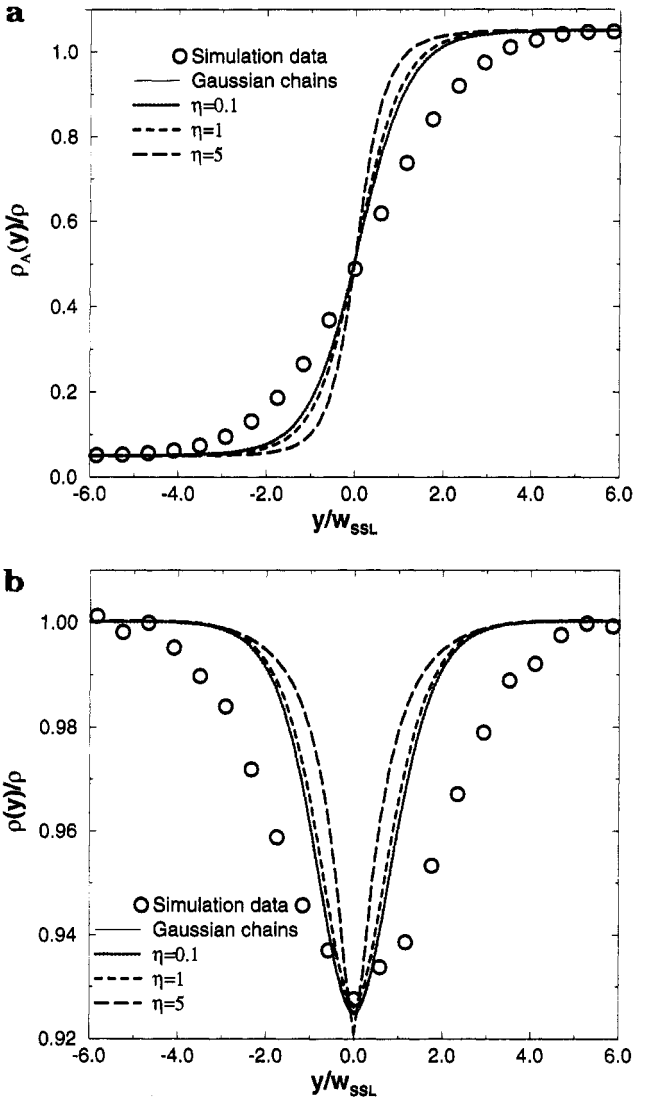

Figure 1. (a) Concentration profile $\rho_A(y)/\rho$ and (b) total density profile $\rho(y)/\rho$ vs y/w_{SSL} (with $w_{SSL} = b/\sqrt{6\chi_{SL}}$) in self-consistent field theory for Gaussian chains (solid line) and semiflexible chains of different chain stiffnesses (dashed/dotted lines), compared with simulation results (circles). The profiles for Gaussian chains overlap with the profile at $\eta = 0.1$. Parameters are $\chi = 0.53$, $\zeta = 4.1$, and $N = 32$.

of the interface.[20] We take it to be constant for a given chain length.

4. Results

Figure 1 shows concentration and density profiles perpendicular to the interface, as predicted by self-consistent field theory for various values of chain stiffness η, and compares them with simulation data. The results look qualitatively similar. Far from the interface, the concentration of A monomers saturates, in the intermediate region; the concentration profile resembles a simple tanh profile. The total density is reduced at the interface, and the depth $\delta\rho$ of the dip in the density profile compares even quantitatively with the value found by simulation.

Apart from this, however, the quantitative agreement of theory and simulation is not very good. The interface appears much broader in the simulation than predicted by self-consistent field theory. The interfacial width is predicted to increase with decreasing chain stiffness (cf. ref 11), but even in the limit of completely flexible Gaussian chains, it is still too small by a factor of

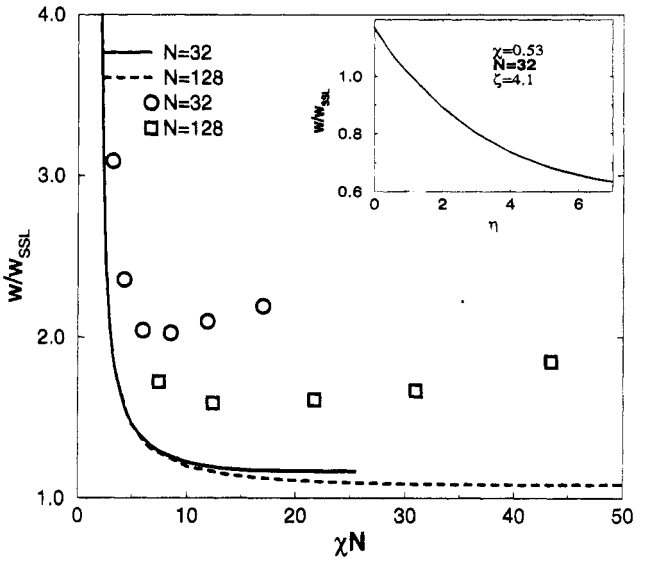

Figure 2. Interfacial width w in units of $w_{SSL} = b/\sqrt{6\chi}$ vs χN at $\zeta = 4.1$ for Gaussian chains (lines), compared with simulation results (symbols), for polymers of lengths $N = 32$ and $N = 128$. The inset shows w/w_{SSL} for semiflexible chains as a function of chain rigidity η at $\chi = 0.53$ and $N = 32$.

roughly 2 compared to the simulations. In order to further explore this discrepancy, we extract a width w from the profiles by fitting the function $\tanh(y/w)$ to the profile $[\rho_A(y) - \rho_B(y)]/\rho$. This width in units of $w_{SSL} = b/\sqrt{6\chi}$ is plotted in Figure 2 vs χN for Gaussian chains, and at fixed $\chi N = 16.96$ vs chain stiffness η for semiflexible chains.

We begin with discussing just the results of self-consistent field theory. For Gaussian chains, the interfacial width is always higher than predicted in the strong segregation limit w_{SSL}. At low values of χN, the interface broadens due to chain end effects; at high values of χ, it broadens due to the effect of finite compressibility. Both effects have been studied separately to low orders in $1/\chi N$ and χ/ζ in the literature. In the specific case of $\chi \approx 0.5$, $N = 128$, and $\zeta = 4$, one expects a broadening of 2% due to chain end effects[5,25] and 5% as an effect of compressibility.[7] Our numerically determined profiles however are broadened by 9%: It is therefore necessary for a quantitative analysis, to perform the full calculation, rather than to rely on low order estimates. With increasing chain stiffness η, the width decreases continuously, as was already obvious from Figure 1.

We compare these results with simulation data at chain lengths $N = 32$ and $N = 128$. There, we note two interesting facts. First, the simulation results for longer chains are closer to the theoretical prediction than for short chains. Second, the reduced width w/w_{SSL} is nonmonotonic in χN. Like in the theoretical prediction, it diverges at the demixing point $(\chi N)_c$ and drops down with increasing χN. But then it reaches a turning point and rises again. As χN increases further, it differs more and more from the theoretical prediction. The turning point is located at $\chi N \approx 6$ for chain lengths $N = 32$, and at $\chi N \approx 12$ for chain lengths $N = 128$, which is about the point where the interfacial width in absolute lattice units gets smaller than ≈6. This happens to be the screening length of the excluded volume interaction,[22] the length scale on which the polymers cannot be safely treated as random walks any more. It is also twice the statistical segment length, and twice the extension of one monomer.

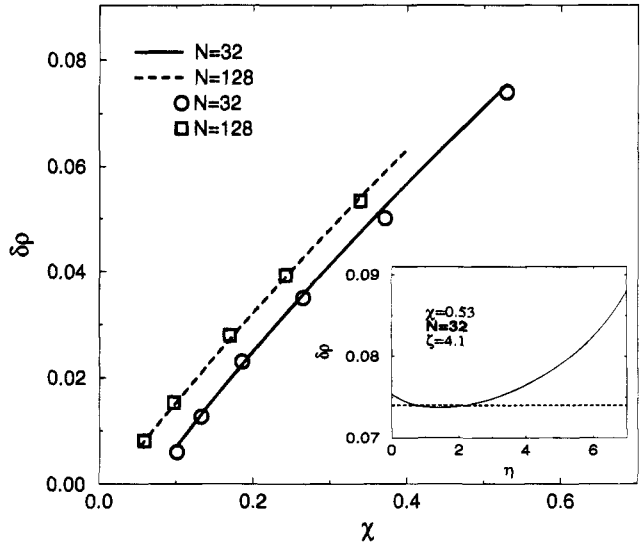

Figure 3. Depth $\delta\rho$ of the dip in the density profile $\rho(y)/\rho$ vs χ for Gaussian chains (lines), compared with simulation results at $N = 32$ (circles) and $N = 128$ (squares), $\zeta = 4.1$. The inset shows $\delta\varrho$ at $\chi = 0.53$ and $N = 32$ as a function of chain stiffness η; the dashed line indicates the value measured by simulation.

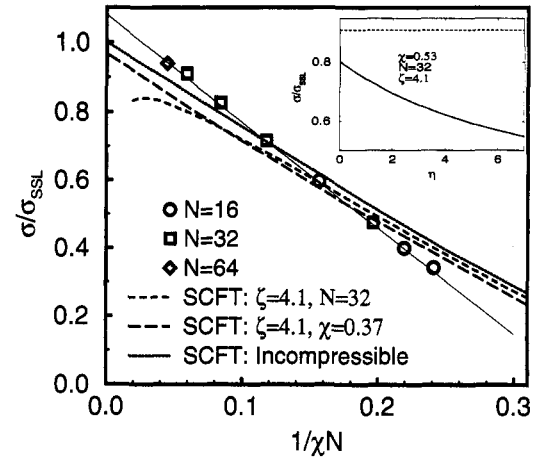

Figure 4. Interfacial tension σ in units of $\sigma_{SSL} = \sqrt{\chi/6}\varrho b k_B T$ vs $1/\chi N$ for Gaussian chains (dashed/dotted lines) and as obtained from simulation (symbols) at $N = 16$, 32, and 64. The solid line is a fit of the simulation data to the linear function $\beta\sigma_0(1 - a_\sigma 2/\chi N)$ with $a_\sigma = 1.44$. The inset shows results for σ/σ_{SSL} vs chain stiffness η with parameters $\chi = 0.53$ and $N = 32$, and the dashed line indicates the value obtained from simulation.

We conclude that the validity of the self-consistent field theory is limited by two different factors. In the limit of low χN, critical fluctuations become important (note that the critical fluctuations shift the demixing point $(\chi N)_c$ by around 20% at chain lengths $N = 32$). At high values of χ, the interface width becomes comparable with microscopic dimensions of the system and the treatment with a simplified coarse-grained free energy functional fails. The larger the region of validity for intermediate χ gets, the longer the chains in the system are. The convergence is, however, very slow, as is obvious from Figure 2. Assuming that a bond in the bond fluctuation model corresponds to roughly three to five chemical monomers in a real polymer (see ref 29), one finds that the limiting effects are still important in systems of real polymers with a degree of polymerization of at least 500, and that they should definitely be kept in mind when comparing self-consistent field theories with experiments.

These effects are most dramatic when looking at the interfacial width. Even though self-consistent field theories fail there quantitatively, they may still be successful in predicting other interfacial properties. We already noted that the depth $\delta\varrho$ of the dip in the concentration profile is reproduced very accurately by the theory. This is further illustrated in Figure 3—over the whole considered range of χN, the simulation results and the theoretical prediction for Gaussian chains are in excellent agreement. Since the dip hardly depends on the chain stiffness η, as long as $\eta \leq 4$, this also holds for semiflexible chains.

The interfacial tension as a function of $1/\chi N$ is plotted for different chain lengths in Figure 4. All simulation data lie very nicely on one single straight line

$$\beta\sigma = \beta\sigma_0\left(1 - a_\sigma \frac{2}{\chi N}\right) \tag{22}$$

with $a_\sigma = 1.44$. This kind of linear behavior to lowest order in $1/\chi N$ has been predicted for incompressible blends by different authors, with $a_\sigma = \ln(2)$, $\pi^2/12$,[25] or 1.35.[5] In a compressible blend, one would not expect such a unique dependence of χN, since one has the additional independent parameter ζ/χ. We calculate the interfacial tension in systems of Gaussian polymers at $\zeta = 4.1$, as a function of χ with fixed $N = 32$, as a function of N with fixed $\chi = 0.37$, and for incompressible blends (following the formalism of Noolandi[10]). Compressibility effects turn out to be of little importance in the parameter range of our simulations. The theoretical results are consistent with a linear decay in $1/\chi N$ with $a_\sigma \approx 1.2$, which is slightly smaller than the value 1.35 suggested by Tang and Freed.[5] For the incompressible blend, our results agree with Shull.[17] Finite compressibility of the blend and nonzero chain stiffness both have the effect of reducing the interfacial tension. In the simulations, the interfacial tension at large χN is higher than would have been expected even in an incompressible system of Gaussian polymers. This is another consequence of the fact that self-consistent field theory underestimates the interfacial width; the interfacial tension is to order zero proportional to the width.

We characterize the system a little further by looking at the chain end distribution (Figure 5). For an A monomer close to the interface, it is entropically more favorable to stick out an end into the minority phase than to build loops into it. Therefore the relative density of A end monomers is increased at the B side of the interface and decreased close to the interface at the A side. The stronger the effect, the sharper the interface gets, and it disappears in the weak segregation limit of small χN, as can be seen in both simulation and self-consistent field theory (Figure 5a). Looking at all polymers, one finds effectively an enrichment of chain ends at the center of the interface and a depletion in the wings of the profile (Figure 5b, cf. ref 3).

As a result of the chain ends being located preferentially close to the interface, whole chains tend to orient themselves parallel to the interface. This is similar to the orientation of chains parallel to a hard wall[30]—the interface acts as a hard wall at high values of χN. In self-consistent field theory, we can study the orientation of whole chains by solving the diffusion equation (13) in the previously determined self-consistent field $\hat{W}_i$ with the initial condition $Q_i(\vec{r},0) = \delta(\vec{r}-\vec{r}_0)$. The statistical weight of a polymer with end-to-end vector $\vec{R}_e = \vec{r}_1 - \vec{r}_0$ and the center at $\vec{R}_c = (\vec{r}_1 + \vec{r}_0)$ is then given by

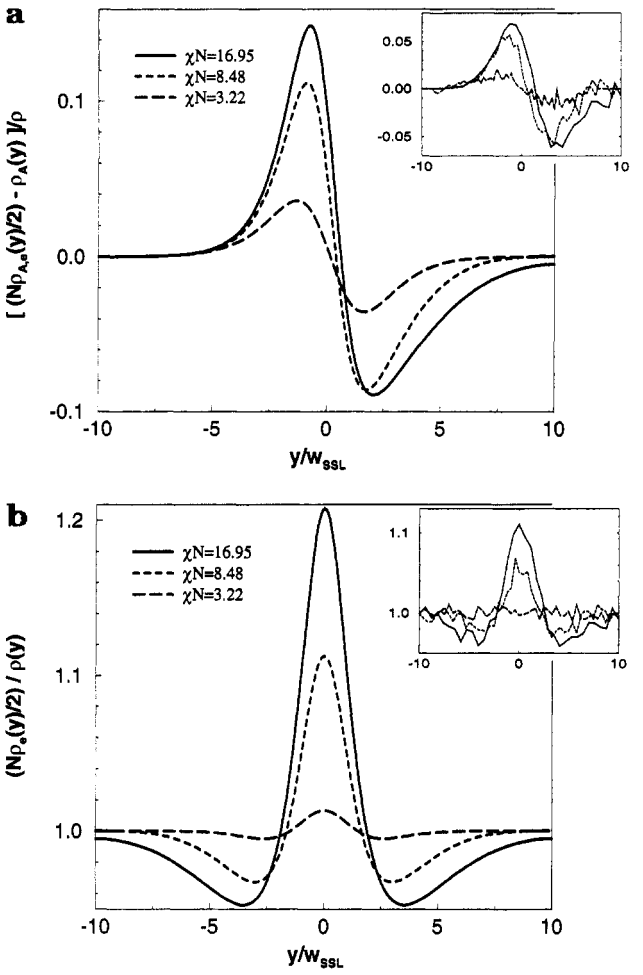

Figure 5. (a) Excess of chain end monomers of type A compared to the total concentration of A monomers across the interface at various values of χN, for Gaussian chains (ζ = 4.1, N = 32). (b) Relative chain end distribution $(N/2)\rho e(y)/\rho$ across the interface at different values of χ, for Gaussian chains, ζ = 4.1, N = 32. The insets show the corresponding Monte Carlo data.

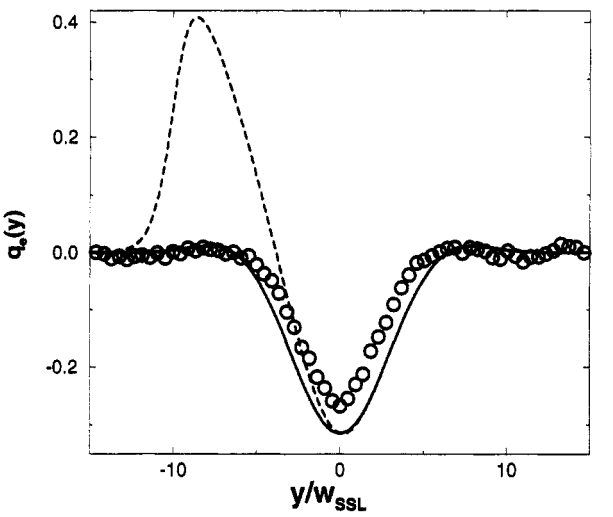

Figure 6. Orientational order parameter of the end-to-end distance $q_e(y)$ vs y/w_{SSL} at χ = 0.53, N = 32, calculated for Gaussian chains (solid line) and compared to simulation results (circles). The dashed line indicates calculated orientational order for only the polymers of type A. Unfortunately, the statistics in the minority region was too poor to allow for a comparison with simulation data.

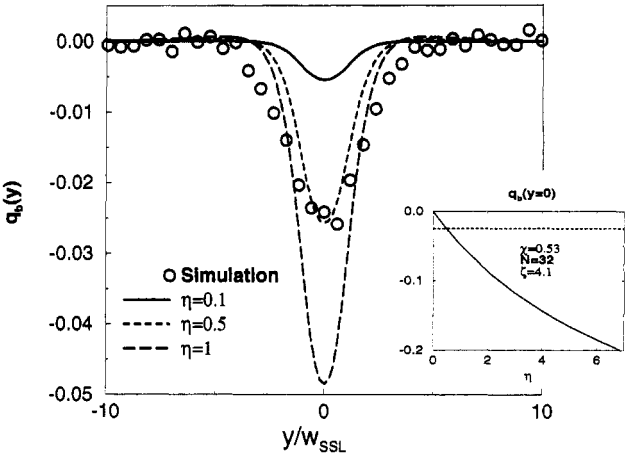

Figure 7. Orientational order parameter of the bond vectors $q_b(y)$ vs y/w_{SSL} at χ = 0.53 and N = 32, calculated for semiflexible chains at various values of stiffness η (lines) and compared to simulation results (circles). The inset shows q_b at the center of the interface as a function of η (solid line); the dashed line indicates the value obtained from simulation.

$Q_i(\vec{r}_1,0)$. As in ref 20, we define an orientation parameter

$$q_e(\vec{R}_c) = \frac{\langle R_{e,y}^2\rangle - {}^1/_2(\langle R_{e,z}^2\rangle + \langle R_{e,x}^2\rangle)}{\langle \vec{R}_e^2\rangle} \qquad (23)$$

where the averages are to be performed for polymers with the center at $\vec{R}_c$. The profile of this orientation parameter obtained for Gaussian chains is compared with simulation results in Figure 6. Self-consistent field theory predicts a slightly too strong alignment. The interface being broader in the simulations than in the theory, it has less of an effect of acting as a hard wall on polymer chains. We note that in contrast to profiles of single monomer properties, the profile of $q_e(y)$ appears narrower in the simulation than in the theory: Compared to the end-to-end distance of a polymer, the interface is a planelike disturbance of negligible width. The width of the profile is thus determined only by the amplitude of the disturbance, which is overestimated by mean field theory.

In the simulations, the orientation of whole chains is found to go along with a much less pronounced orientation of single bonds. In analogy to the orientation parameter q_e, one can define a bond orientation parameter q_b, which can be compared with the average orientation of the tangent vector $\vec{u}$ in the self-consistent field theory for semiflexible chains: $q_b \hat{=} {}^1/_2(3\langle u_y^2\rangle - 1)$. The results are shown in Figure 7. In self-consistent field theory as well as in the simulations, $\vec{u}$ is found to be preferably oriented parallel to the interface. The degree of alignment $|q_b(0)|$ vanishes in the limit of zero rigidity η. Optimal agreement with the simulations is reached at $\eta \approx 0.5$. At stiffness η = ${}^1/_2$, the statistical segment length $b = \sqrt{2\eta}a$ is identical to the "monomer length" a, hence adjacent monomers are essentially uncorrelated. The main difference between a Gaussian chain and a semiflexible chain with such a small rigidity is that the effective monomer has a fixed length a, whereas the statistical segment has not. This is indeed roughly the situation encountered in the bond fluctuation model. We obtain an effective monomer length $a \approx 3$, which agrees reasonably well with the average bond length in the bond fluctuation model, 2.64 lattice units.

5. Summary

We have compared the predictions of self-consistent field theories for interfacial properties in a symmetric polymer blend with the results of extensive Monte Carlo simulations. For this purpose, we have solved numerically, without further approximations, the self-consistent field equations for flexible polymers and presented a formalism, which enabled us to solve them for semiflexible polymers as well. The validity of self-consistent field theories is limited by critical fluctuations on the one hand and by the interfacial width getting small compared to the microscopic length scales of the system on the other hand. We found that the effect of those limiting factors is quite dramatic as one looks at monomeric profiles, in particular at the width of the interface. But even when it fails there, self-consistent field theories are still remarkably successful in quantitatively predicting other properties of the interface. Qualitatively, many characteristics of the interface could be reproduced, like whole chain and single bond orientation profiles and chain end distributions. Although we have no conclusive evidence, our results indicate that the microscopic length scale, which limits the applicability of the self-consistent field theory in the low-temperature regime might be related to the screening length of the excluded volume. This hypothesis could be tested by comparing with simulations at a different bulk density Φ, where the screening length is different. One could possibly improve the theory by accounting for the self-avoiding character of polymers on small length scales in the path integral (1). At very low temperatures, however, every field theory will fail, as typical length scales become comparable with the dimensions of the monomers.

Acknowledgment. We are grateful to K. Binder for suggesting the problem, numerous discussions, and careful reading of the manuscript and to W. Oed for invaluable help in optimizing the program for the Cray T3D. F.S. has greatly benefited from discussions with M. Matsen. M.M. received partial support from the Deutsche Forschungsgemeinschaft under Grant No. Bi314/3. Generous access to the Cray T3D at CINECA and EPFL is acknowledged.

References and Notes

(1) De Gennes, P.-G. *Scaling Concepts in Polymer Physics*; Cornell University Press: Ithaca, NY, 1953.
(2) Binder, K. *J. Chem. Phys.* **1983**, *79*, 6387; *Phys. Rev. A* **1984**, *29*, 341.
(3) See, for example: *Physics of Polymer Surfaces and Interfaces*; Sanchez, I. C., Ed.; Butterworth-Heinemann: Boston, 1992.
(4) De Gennes, P.-G. *J. Chem. Phys.* **1980**, *72*, 4756; Roe, R-J. *Macromolecules* **1986**, *19*, 728.
(5) Tang, H.; Freed, K. F. *J. Chem. Phys.* **1991**, *94*, 6307.
(6) Lifschitz, M.; Freed, K. F. *J. Chem. Phys.* **1993**, *98*, 8994.
(7) Helfand, E.; Tagami, Y. *J. Polym. Sci. B* **1971**, *9*, 741; *J. Chem. Phys.* **1971**, *56*, 3592; **1972**, *57*, 1812. Helfand, E.; Sapse, A. M. *J. Chem. Phys.* **1975**, *62*, 1327.
(8) Helfand, E. *J. Chem. Phys.* **1975**, *62*, 999.
(9) Scheutjens, J. M. H. M.; Fleer, G. J. *J. Chem. Phys.* **1979**, *83*, 1619.
(10) Hong, K. M.; Noolandi, J. *Macromolecules* **1981**, *14*, 727; Matsen, M. W.; Schick, M. *Phys. Rev. Lett.* **1994**, *72*, 2660.
(11) Morse, D. C.; Fredrickson, G. H. *Phys. Rev. Lett.* **1994**, *73*, 3235.
(12) Deutsch, H.-P.; Binder, K. *Macromolecules* **1992**, *25*, 6214; *J. Phys. II* **1993**, *3*, 1049.
(13) Holyst, R.; Vilgis, T. A. *J. Chem. Phys.* **1993**, *99*, 4835; Lifschitz, M.; Dudowicz, J.; Freed, K. F. *J. Chem. Phys.* **1994**, *100*, 3957.
(14) Schwahn, D.; Meier, G.; Mortensen, K.; Janssen, S. *J. Phys. II* **1994**, *4*, 837.
(15) Shull, K. R.; Kramer, E. J. *Macromolecules* **1990**, *23*, 4769.
(16) Shull, K. R.; Mayes, A. M.; Russell, T. P. *Macromolecules* **1993**, *26*, 3929.
(17) Shull, K. R. *Macromolecules* **1993**, *26*, 2346.
(18) Wijmans, C. M. To be published.
(19) Reiter, J.; Zifferer, G.; Olaj, O. F. *Macromolecules* **1990**, *23*, 224.
(20) Müller, M.; Binder, K.; Oed, W. *Faraday Trans.*, in press.
(21) Carmesin, I.; Kremer, K. *Macromolecules* **1988**, *21*, 2819.
(22) Paul, W.; Binder, K.; Heermann, D. W.; Kremer, K. *J. Phys. II* **1991**, *1*, 37.
(23) Müller, M.; Paul, W. *J. Chem. Phys.* **1993**, *100*, 719.
(24) Leibler, L. *Macromolecules* **1982**, *15*, 1283.
(25) Helfand, E.; Bhattacharjee, S. M.; Fredrickson, G. H. *J. Chem. Phys.* **1989**, *91*, 7200; Broseta, D.; Fredrickson, G. H.; Helfand, E.; Leibler, L. *Macromolecules* **1990**, *23*, 132.
(26) Dudowicz, J.; Freed, K. F. *Macromolecules* **1990**, *23*, 1519.
(27) Deutsch, H.-P.; Dickman, R. *J. Chem. Phys.* **1990**, *93*, 8983.
(28) Saito, N.; Takahashi, K.; Yunoki, Y. *J. Phys. Soc. Jpn.* **1967**, *22*, 219.
(29) Baschnagel, J.; Binder, K.; Paul, W.; Laso, M.; Suter, U.; Batoulis, I.; Jilge, W.; Bürger, T. *J. Chem. Phys.* **1991**, *95*, 6014.
(30) Kumar, S. K.; Vacatello, M.; Yoon, D. Y. *J. Chem. Phys.* **1988**, *89*, 5206; *Macromolecules* **1990**, *23*, 2189; ten Brinke, G.; Ausserre, D.; Haddzioannou, G. *J. Chem. Phys.* **1988**, *89*, 4374; Yethiraj, A.; Hall, C. K. *Macromolecules* **1990**, *23*, 1865; Wang, J. S.; Binder, K. *J. Phys. II* **1991**, *1*, 1583.

MA9507047